



HAL
open science

Multiphoton imaging of host-pathogen interactions

Keira Melican, Agneta Richter-Dahlfors

► **To cite this version:**

Keira Melican, Agneta Richter-Dahlfors. Multiphoton imaging of host-pathogen interactions. *Biotechnology Journal*, 2009, 4 (7), pp.804-n/a. 10.1002/biot.200800347 . hal-00482926

HAL Id: hal-00482926

<https://hal.science/hal-00482926>

Submitted on 12 May 2010

HAL is a multi-disciplinary open access archive for the deposit and dissemination of scientific research documents, whether they are published or not. The documents may come from teaching and research institutions in France or abroad, or from public or private research centers.

L'archive ouverte pluridisciplinaire **HAL**, est destinée au dépôt et à la diffusion de documents scientifiques de niveau recherche, publiés ou non, émanant des établissements d'enseignement et de recherche français ou étrangers, des laboratoires publics ou privés.



Multiphoton imaging of host-pathogen interactions

Journal:	<i>Biotechnology Journal</i>
Manuscript ID:	BIOT-2008-0347.R3
Wiley - Manuscript type:	Review
Date Submitted by the Author:	23-Mar-2009
Complete List of Authors:	Melican, Keira; Karolinska Institutet, Department of Neuroscience Richter-Dahlfors, Agneta; Karolinska Institutet, Department of Neuroscience
Keywords:	Infection , intravital microscopy, multiphoton, two-photon , pathogen



Review

Review

Multiphoton imaging of host-pathogen interaction

The Hengstberger Symposium 'Imaging Host-Pathogen Interaction'

Heidelberg September 2008

Keira Melican^{1,2} and Agneta Richter-Dahlfors^{1,2}

¹Swedish Medical Nanoscience Center, ²Department of Neuroscience,

Karolinska Institutet, SE 171-77 Sweden

Correspondence:

Professor Agneta Richter-Dahlfors

Swedish Medical Nanoscience Center

Karolinska Institutet

Department of Neuroscience

Retzius väg 8

17177 Stockholm

Sweden

Fax: +468311101

Phone: +46852487425

Email: Agneta.Richter.Dahlfors@ki.se

Keywords: Infection, intravital, multiphoton, two-photon microscopy, live imaging.

Abbreviations: MPM (Multiphoton microscopy), UPEC (uropathogenic *Escherichia*

coli), LPS (lipopolysaccharide), GFP (green fluorescent protein), VSV (vesicular

stomatitis virus)

1
2
3 284
5 296
7
8 **Abstract**9
10 31 Studying the events which occur when a pathogen comes into contact with its host is the11
12 32 basis of the field of infection biology. Over the years, work in this area has revealed13
14 33 many facets of the infection process including attachment, invasion and colonization by15
16 34 the pathogen, as well as the host responses, such as the triggering of the immune system.17
18 35 Recent advancements in imaging technologies, such as multiphoton microscopy, mean19
20 36 that the field is in the process of taking another big leap forward. Multiphoton21
22 37 microscopy allows for cellular level visualization of the real-time dynamics of infection23
24 38 within the living host. The use of live animal models means that all the interplaying25
26 39 factors of an infection, such as the influences of the immune, lymphatic and vascular27
28 40 systems can be accounted for. This review outlines the developing field of multiphoton29
30 41 microscopy in pathogen-host interaction, highlighting a number of new insights which31
32 42 have been 'brought to light' using this technique.33
34 4335
36 44
37
38
39
40
41
42
43
44
45
46
47
48
49
50
51
52
53
54
55
56
57
58
59
60

1
2
3 45 **Introduction.**
4

5 46 The interaction between pathogens and their hosts is a complex and dynamic event. An
6
7 47 infection is accompanied by responses from both the pathogen and the host and it is the
8
9
10 48 balance between these responses which defines the infection outcome. In studying this
11
12
13 49 complex interplay, imaging technologies can play a vital role [1]. Fluorescence based
14
15 50 imaging techniques have long been a favorite in the infection field due the ability to
16
17
18 51 differentially label the pathogens and the cells with which they interact. While many
19
20 52 valuable studies have been carried out in cell culture models, the development of new
21
22 53 imaging technologies is now enabling experiments to be performed within the full
23
24 54 complexity of the host tissue. The host tissue is far more heterogeneous than cell culture
25
26
27 55 and understanding the interaction between the different cells types in response to
28
29 56 infection is crucial to understanding the infectious process [2]. Confocal microscopy,
30
31 57 both laser scanning (LSCM) and others such as spinning disk (SDCM) [3] allows for 3D
32
33 58 imaging providing the ability to address spatial aspects of tissue infection [4]. In a
34
35 59 majority of cases, however, specimens for confocal microscopy are dead, fixed tissues
36
37 60 which can only give a single time point for any particular infection. In live animal
38
39 61 models, the imaging depth limitations of confocal microscopy means that they may only
40
41 62 be utilized for very superficial sites of infections [5, 6]. With the recent advancements in
42
43 63 intravital imaging technologies, however, we are now at a point where we can overcome
44
45 64 these limitations as well as add the 4th dimension of infection; time, to enable
46
47 65 visualization of the true dynamics of tissue infection. In recent years a number of very
48
49 66 good technique focused reviews have been published on the subject of imaging in
50
51 67 infection [1-3, 7], this review aims to focus on recent applications of multiphoton-
52
53
54
55
56
57
58
59
60

1
2
3 68 microscopy in pathogen-host interaction.
4
5

6 69

70 **Multiphoton Microscopy**

71 Multiphoton microscopy (MPM) is an increasingly popular technique which
72 overcomes a number of the limitations of confocal microscopy while offering almost
73 comparable resolution [8]. The principle of MPM lies in the use of non-linear optical
74 processes [9]. While similar to LSCM in regards to the laser scanning of the specimen,
75 MPM uses a long wavelength (infrared) light to excite only the fluorophores in a specific
76 femtoliter sample volume at the focal plane [10]. To enable the excitation of the
77 fluorophores in the sample volume using lower energy, longer wavelengths of light, the
78 photons energies must be concentrated in space and time, 'crowded', so that two photons
79 interact with the fluorophore simultaneously (within $\sim 10^{-16}$ s) to produce sufficient
80 excitation energy [11]. Spatial concentration can be achieved by focusing the excitation
81 laser through a high numerical aperture objective, while concentration in time is achieved
82 by using ultra short (< 1ps) pulses to create the required excitation intensities
83 while maintaining a relatively low average power [8, 12]. The simultaneous absorption of
84 the two photons excites the fluorophore to its excitation state from which it will emit its
85 characteristic Stokes shifted wavelength [10] (Figure 1). This form of imaging holds a
86 number of advantages for intravital use. Wavelengths in the 700-1000nm range, as
87 commonly used for MPM, are generally considered to produce negligible photodamage,
88 resulting in improved cell viability [8]. Due to a reduction in Rayleigh scattering these
89 longer wavelengths can also penetrate further into biological tissue [13]. By focusing the
90 excitation to such a small volume, photobleaching and damage in the tissue is minimized

1
2
3 91 as the majority of the tissue volume is not in an excited state [11]. This feature also
4
5 92 means that no excitation occurs outside the specified region, in effect giving no out-of-
6
7
8 93 focus signal. The lack of out-of-focus absorption means more of the excitation light
9
10 94 reaches the target and also that all emitted photons are relevant. The use of detection
11
12 95 methods which capture as many emitted photons as possible can help increase the
13
14 96 sensitivity of fluorescence detection [11]. An additional advantage of MPM is the
15
16 97 phenomenon of second harmonic generation (SHG), a process of non-linear light
17
18 98 scattering. SHG occurs when multiple photons simultaneously interact with certain
19
20 99 proteins, such as those in the extracellular matrix, to produce radiation at half the
21
22 100 wavelength of the incident light [8, 14]. This means certain structures, e.g. collagen, can
23
24
25 101 be visualized without the need for staining or labeling. An example of SHG can be seen
26
27 102 in Figure 4. Despite its numerous advantages, there are drawbacks and/or limitations to
28
29 103 multiphoton microscopy which must be taken into account when designing experiments.
30
31 104 As described above, multiphoton excitation can reduce the overall levels of
32
33 105 photodamage, but it has been shown that instead of an intensity-squared relationship
34
35 106 between excitation power and the photobleaching rate, multiphoton excitation may
36
37 107 demonstrate higher order photobleaching at the focal site [15]. Linear absorption or the
38
39 108 infra-red excitation light can also result in some level of tissue heating, particularly in
40
41 109 pigmented tissue containing single photon absorbers such as hemoglobin or melanin [16,
42
43 110 17]. In our hands repeated imaging of a single site sometimes lead to subtle changes in
44
45 111 tissue homeostasis, such as effecting the cellular endocytosis pathways (unpublished
46
47 112 data), and as such must be carefully controlled to limit these effects. Speed of image
48
49 113 capture can also be a limitation depending on experimental aim. The relative slow
50
51
52
53
54
55
56
57
58
59
60

1
2
3 114 scanning speed of a single beam is now being improved upon by the use of a multifocal
4
5 115 multiphoton set-up in which the incoming laser-beam can be split into numerous separate
6
7
8 116 beams [18, 19]. This forms the basis for the recently developed TriM microscope system,
9
10 117 which can increase the number of fluorescence photons per time unit without increasing
11
12 118 photo damage by parallelizing the excitation process.

15 119 Organs such as the brain, kidney and lymph nodes are well established intravital
16
17 120 models while others such as the liver and spleen are fast catching up. Of major
18
19 121 importance when choosing MPM for the study of pathogen-host interaction is
20
21 122 accessibility to the organ of interest. Organs which can be easily accessed or exteriorized
22
23 123 without affecting structure and function are ideal [20]. Physiological processes such as
24
25 124 respiration, peristalsis and heart beat can produce movement artifacts which can limit the
26
27 125 usability of some organs. These issues can often be overcome through innovative surgical
28
29 126 and experimental techniques. A common compromise to eliminate these movement and
30
31 127 accessibility issues is to use tissue explants. Tissue explants are organs which are
32
33 128 surgically removed and then maintained *in vitro* [21, 22]. Tissue explants have
34
35 129 advantages over cell culture such as their heterogeneity, three dimensional structure and
36
37 130 ease of accessibility and manipulation. They do not however, fully reflect the live
38
39 131 situation due to the difficulty in maintaining a physiologically relevant environment and
40
41 132 their lack of systemic influences, limiting their use in studies looking at factors such as
42
43 133 blood flow. The presence of all interplaying physiological factors, such as the vascular,
44
45 134 lymphatic and nervous systems, in the live animal model means the influences and
46
47 135 interplays of all these systems can be accounted for. The live animal model also enables
48
49 136 the study of systemic and remote responses to a local infection, giving a more complete
50
51
52
53
54
55
56
57
58
59
60

1
2
3 137 picture of the pathology. Good surgical techniques are essential for a number of reasons
4
5 138 in MPM of live animal models, not least to enable efficient exteriorization of the tissue of
6
7
8 139 interest. Maintenance of a physiological state in terms of fluid levels, temperature, blood
9
10 140 pressure and anesthesia are all factors which must be taken into account.
11

12
13 141

14 142 **Studying pathogen-host interaction with multiphoton microscopy**

15
16
17 143 Intravital MPM has primarily been pioneered in physiological studies, with much
18
19
20 144 of the early developmental work performed in the brain [12, 23-25]. It is only in recent
21
22 145 years that it has been adopted into infection biology. While the use of live pathogens is a
23
24 146 relatively recent advancement, using MPM to study the inflammatory response, using
25
26
27 147 immunomodulatory microbial components such as lipopolysaccharide (LPS) has been
28
29 148 reported. A number of informative reviews have been published regarding the use of
30
31 149 MPM in immunology, and we would like to direct readers towards these for more in-
32
33 150 depth discussion [21, 22, 26-28]. Proof of principle experiments using intact pathogens
34
35 151 showed the suitability of MPM for imaging events such as amoeboid motility of
36
37
38 152 *Entamoeba histolytica* [29] in infected tissue and fungal infection with *Cryptococcus*
39
40 153 *neoformans* in the brain [2]. So while still in its infancy, the use of MPM to study
41
42 154 infection is growing rapidly. The potential of the technique for the study of pathogen-host
43
44 155 interaction is rapidly becoming apparent, as is also outlined in a few other very recent
45
46 156 reviews on the topic [30-32].
47
48
49

50 157

51 158 **Bacteria**

52
53
54
55 159 In the course of physiological MPM studies bacterial components, such as LPS, have
56
57
58
59
60

1
2
3 160 been used to study pathophysiology, such as in kidney injury during sepsis [33, 34].
4
5 161 Cecal ligation and LPS injections were shown to effect renal toll-like receptor 4
6
7
8 162 expression in a live sepsis model [33], while LPS induced exotoxemia was shown to be
9
10 163 ameliorated by activated protein kinase C [34]. These reports focused on the secondary
11
12 164 physiological injury caused or exacerbated by bacterial components rather than the
13
14 165 infection process itself. In collaboration with the intravital renal imaging specialists at the
15
16 166 George M. O'Brien Center for Advanced Renal Microscopic Analysis at the Indiana
17
18 167 Center for Biological Microscopy, our group utilized intravital MPM to follow the
19
20 168 progression of bacterial infection in the kidney [35]. To enable visualization of
21
22 169 uropathogenic *Escherichia coli* (UPEC) *in vivo*, where standard labeling techniques are
23
24 170 impracticable, a clinical isolate expressing the green fluorescent protein GFP⁺ [36] from a
25
26 171 single chromosomal copy was constructed. This construct had a number of advantages
27
28 172 for long-term intravital studies; as the GFP⁺ expression was under the control of a
29
30 173 constitutively active promoter, the protein was expressed in all tissue environments. The
31
32 174 chromosomal location also removed the risks of plasmid rejection or toxic GFP⁺ levels.
33
34 175 Delivery of the bacteria to enable optimal spatial and temporal resolution was achieved
35
36 176 by micro-infusion directly into superficial tubule lumens in the renal cortex. Marking of
37
38 177 the site, by co-injection of a small molecular weight fluorescent dextran which is
39
40 178 endocytosed by the proximal tubules cells [35], enables visualization from the first hours
41
42 179 of infection, when bacterial numbers are very low, through to days after (Figure 2).
43
44 180 Visualization of the first hours of infection facilitated the identification of events such as
45
46 181 the early stages of bacterial colonization and vascular dysfunction [7]. Using MPM we
47
48 182 have shown that tubular bacterial infection triggers an epithelial response that affected
49
50
51
52
53
54
55
56
57
58
59
60

1
2
3 183 signaling and local tissue oxygen tension, and resulted in clotting of local capillaries
4
5 184 within the first 4-5 h of infection. This response was identified as an innate immune
6
7
8 185 response as it was shown to be essential for the prevention of systemic bacterial
9
10 186 dissemination and fatal sepsis [37]. These results highlight the unique ability of the live
11
12 187 model to identify vascular biology events such as changes in tissue oxygen tension and
13
14 188 blood flow in the hours immediately following infection and identifying previously
15
16 189 unrecognized pathophysiology. These studies also identified the dynamics of immune
17
18 190 cell migration into the tissue and chemotaxis of neutrophils out into the lumen of
19
20 191 proximal tubules where the bacteria were located [35]. Current work in our laboratory is
21
22 192 using the same technology to begin looking more closely at bacterial adaptation to the
23
24 193 changing *in vivo* microenvironment during infection (Melican et al, unpublished data).
25
26 194 The ability to study both host and pathogen responses to infection *in vivo* means MPM is
27
28 195 helping advance the field of 'Cellular Microbiology' towards 'Tissue Microbiology'. An
29
30 196 example of MPM imaging of live kidney infection can be seen in Figure 2.
31
32
33
34
35

36 197 Other studies looking at bacterial infection have also utilized the unique 'all-
37
38 198 inclusive' nature of the live model to look at infection and particularly the host response
39
40 199 to it. Both live animal and explant MPM imaging of the terminal ileum of mice has
41
42 200 shown dendritic cell extension in response to infection with *Salmonella typhimurium*. It
43
44 201 was demonstrated how epithelial toll like receptor signaling induced active dendritic cell
45
46 202 (DC) sampling of the gut lumen [38]. Egen *et al* used intravital MPM to identify a role
47
48 203 for liver Kupffer cells in the capture of blood-borne *mycobacteria* and the initiation of
49
50 204 granuloma formation [39]. An investigation into the dynamics of innate immune cell
51
52 205 trafficking during the early phase (1-4 h) of *Listeria monocytogenes* induced
53
54
55
56
57
58
59
60

1
2
3 206 inflammation was performed using MPM on the mouse footpad [40]. Aoshi *et al* have
4
5 207 recently published a study performed using explanted spleen which suggests that splenic
6
7 208 dendritic cells rapidly deliver intracellular *Listeria monocytogenes* to the T cell areas of
8
9 209 the white pulp to initiate CD8+ T cell responses [41]. MPM of infection in both live
10
11 210 animal models and tissue explants highlights the advantages of MPM for study of the
12
13 211 dynamic responses of the host to bacterial infection.
14
15
16
17
18
19

20 213 **Parasites**

21
22 214 Parasitic infections are an ideal model for intravital imaging. The dynamic readouts
23
24 215 offered by these techniques lend themselves very well to the study of both the parasitic
25
26 216 lifestyle and the immune response to such infections. Imaging of the different parasite
27
28 217 stages across the *Plasmodium* life cycle, has described a number of dynamic events [42-
29
30 218 44]. Looking at the very early stages of infection in the mouse ear, Amino *et al* have
31
32 219 used high speed confocal microscopy to study the fate of *Plasmodium* sporozoites
33
34 220 following a mosquito bite [5, 6]. Confocal microscopy and conventional epi-fluorescence
35
36 221 microscopy was also used to look at the liver stages of *Plasmodium* infection either
37
38 222 through explants or live preparation [45-47]. In an MPM based study, the malarial
39
40 223 pigment hemozoin (HZ) has been shown to shown to affect T cell interaction with
41
42 224 dendritic cells in isolated lymph nodes [48]. MPM has also been utilized in the study of
43
44 225 *Leishmania* parasitic infection. Infection with *Leishmania major* was shown to effect the
45
46 226 localization of natural killer cells in live lymph nodes as well as their expression of
47
48 227 interferon γ [49]. MPM imaging of *Leishmania m.* infection in the mouse ear has shown
49
50 228 how early infiltrating neutrophils take up a significant fraction of infecting parasites
51
52
53
54
55
56
57
58
59
60

1
2
3 229 (Figure 3). These parasites remain viable and could contribute to the establishment and
4
5
6 230 progression of the disease. Depletion of neutrophils was also shown to hinder rather than
7
8 231 enhance parasitic infection [50]. These papers indicate how the parasite interacts with and
9
10 232 affects the cells of the innate immune system. Intravital observations by MPM are of
11
12 233 great help in elucidating the complexity of these interactions. Similarly, MPM of
13
14 234 explanted lymph nodes visualized the effect of the parasite *Toxoplasma gondii* on
15
16 235 neutrophil behavior, beautifully demonstrating the swarming behavior of these cells in
17
18 236 the lymph node [51].
19
20
21
22
23

24 238 **Viruses**

26
27 239 Intravital imaging has also been used to study viral infections. In a study
28
29 240 demonstrating both the dynamic and comprehensive nature of the live animal models,
30
31 241 Junt *et al* injected fluorescently labeled inactivated, vesicular stomatitis virus (VSV) into
32
33 242 the footpad of mice and then imaged live the draining lymph node showing virus arrival
34
35 243 and localization [52] (Figure 4). This work also indicated a dual physiological function of
36
37 244 CD169+ macrophages during infection, acting both as an innate ‘flypaper’ to prevent
38
39 245 spread of lymph-borne viruses and in the initiation of the humoral immune response. In a
40
41 246 similar study Hickman *et al* also studied how virus particles are handled in the draining
42
43 247 lymph nodes, looking at both vaccinia, a large DNA virus and VSV, a small RNA virus
44
45 248 [53]. This study also showed the initiation of the adaptive immune response and how
46
47 249 antigen presentation in the lymph node periphery, as opposed to the lymphocyte exit
48
49 250 sites, has a leading role in activation of antiviral CD8+ T cell. These two studies highlight
50
51 251 how MPM can help in the study of pathogen interaction with, and initiation of, the innate
52
53
54
55
56
57
58
59
60

1
2
3 252 and adaptive immune responses. A very recent study using MPM to image the meninges
4
5 253 of a mouse infected with Lymphocytic choriomeningitis virus (LCMV), showed how the
6
7
8 254 immune response may affect other physiological systems such as the vasculature.
9
10 255 Recruitment of myelomonocytic cells caused leakage in the local meningeal vascular,
11
12 256 breakdown of the blood-brain barrier, and lead to fatal seizures [54]. This study also
13
14
15 257 demonstrated the use of a thinned skull window, a common technique in neuroscience,
16
17 258 allowing for extended imaging over a number of days with no repeated surgical
18
19 259 intervention required. Viruses have also been used as delivery vectors, as exemplified by
20
21 260 adenoviral-mediated gene transfer to introduce fluorescent proteins for intravital MPM
22
23 261 [55].
24
25
26
27 262

29 263 **Conclusions and future directions**

31 264 Imaging within the living organ is becoming more and more accessible to researchers
32
33 265 looking at pathogen-host interaction. The dynamics of infection and the host response to
34
35 266 it are now able to be visualized, often in real-time, in the most physiologically relevant
36
37 267 setting. As the technology advances, with the development of more ‘turn-key’ systems
38
39 268 enabling ease of use, as well as optical advancements such as the endoscopic models [56,
40
41 269 57], its usability will increase. These models will open up numerous new lines of
42
43 270 research, as physiological responses which are unable to be studied *in vitro* or in static
44
45 271 models are identified. The ability to be able to combine molecular quantification with
46
47 272 visualized events will help give an *in vivo* role to a number of events seen *in vitro*. One
48
49 273 expanding field combining imaging with molecular quantification is the development of
50
51 274 new fluorescent probes. Fluorescently labeled dextrans have allowed for functional
52
53
54
55
56
57
58
59
60

1
2
3 275 studies on numerous physiological processes in the kidney [58]. Photoswitchable
4
5 276 fluorescent proteins such as Kaede [59] and Dendra [60] allow for switching of
6
7
8 277 fluorescent wavelengths after photoactivation, which can be used for tracking certain
9
10 278 populations of labeled cells. This technique, combined with the implantation of a chronic
11
12 279 imaging window and intravital confocal microscopy, has been recently described in an
13
14 280 elegant paper describing cancer cell metastasis [61] . The use of functionalized quantum
15
16 281 dots is another developing field which may allow imaging based sensing of cellular
17
18 282 environments and delivery of ligands and other factors *in vivo* [62, 63]. Bacterial genetic
19
20 283 mutants and the like will also help address the precise role of certain bacterial virulence
21
22 284 factors in the *in vivo* setting, roles which may be previously unimaginable. The study of
23
24 285 drug treatment regimes within the living model in high resolution may demonstrate both
25
26 286 the effectiveness of treatment, and also the drugs mode of action. In conclusion intravital
27
28 287 MPM offers great opportunities for researchers working on pathogen-host interaction to
29
30 288 move their studies directly into the host without compromising on spatial or temporal
31
32 289 resolution.
33
34
35
36
37
38
39
40

41 **Acknowledgments**

42
43 292 The authors would like to thank The Swedish Research Council – Medicine,
44
45 293 Jordbruksverket and Svenska Läkaresällskapet for financial support of our work. The
46
47 294 authors have declared no conflict of interest.
48
49
50
51
52
53
54
55
56
57
58
59
60

297 References

- 298 [1] Frischknecht, F., Renaud, O., Shorte, S. L., Imaging Today's Infectious Animalcules.
299 *Curr Opin Microbiol* 2006, 9, 297-306.
- 300 [2] Roux, P., Munter, S., Frischknecht, F., Herbomel, P., Shorte, S. L., Focusing Light on
301 Infection in Four Dimensions. *Cell Microbiol* 2004, 6, 333-343.
- 302 [3] Enninga, J., Sansonetti, P., Tournebize, R., Roundtrip Explorations of Bacterial
303 Infection: From Single Cells to the Entire Host and Back. *Trends Microbiol* 2007, 15,
304 483-490.
- 305 [4] Richter-Dahlfors, A., Buchan, A. M., Finlay, B. B., Murine Salmonellosis Studied by
306 Confocal Microscopy: Salmonella Typhimurium Resides Intracellularly inside
307 Macrophages and Exerts a Cytotoxic Effect on Phagocytes in Vivo. *J Exp Med* 1997,
308 186, 569-580.
- 309 [5] Amino, R., Franke-Fayard, B., Janse, C., Waters, A., *et al.*, Imaging Parasites in Vivo,
310 in: Shorte, S. L., Frischknecht, F. (Eds.), *Imaging Cellular and Molecular Biological*
311 *Functions*, Springer, Heidelberg 2007, pp. 345-364.
- 312 [6] Amino, R., Thiberge, S., Martin, B., Celli, S., *et al.*, Quantitative Imaging of
313 Plasmodium Transmission from Mosquito to Mammal. *Nat Med* 2006, 12, 220-224.
- 314 [7] Mansson, L. E., Melican, K., Molitoris, B. A., Richter-Dahlfors, A., Progression of
315 Bacterial Infections Studied in Real Time--Novel Perspectives Provided by Multiphoton
316 Microscopy. *Cell Microbiol* 2007, 9, 2334-2343.
- 317 [8] Zipfel, W. R., Williams, R. M., Webb, W. W., Nonlinear Magic: Multiphoton
318 Microscopy in the Biosciences. *Nat Biotechnol* 2003, 21, 1369-1377.

- 1
2
3 319 [9] Bullen, A., Microscopic Imaging Techniques for Drug Discovery. *Nat Rev Drug*
4
5 320 *Discov* 2008, 7, 54-67.
6
7
8 321 [10] Hazelwood, K. L., Olenych, S. G., Griffin, J. D., Cathcart, J. A., Davidson, M. W.,
9
10 322 Entering the Portal: Understanding the Digital Image Recorded through a Microscope, in:
11
12 323 Shorte, S. L., Frischknecht, F. (Eds.), *Imaging Cellular and Molecular Biological*
13
14 324 *Functions*, Springer, Heidelberg 2007, pp. 3-45.
15
16
17 325 [11] Piston, D. W., Imaging Living Cells and Tissues by Two-Photon Excitation
18
19 326 Microscopy. *Trends Cell Biol* 1999, 9, 66-69.
20
21
22 327 [12] Helmchen, F., Denk, W., Deep Tissue Two-Photon Microscopy. *Nat Methods* 2005,
23
24 328 2, 932-940.
25
26
27 329 [13] Theer, P., Hasan, M. T., Denk, W., Two-Photon Imaging to a Depth of 1000 Microm
28
29 330 in Living Brains by Use of a Ti:Al₂O₃ Regenerative Amplifier. *Opt Lett* 2003, 28, 1022-
30
31 331 1024.
32
33
34 332 [14] Kaestner, L., Lipp, P., Towards Imaging the Dynamics of Protein Signalling, in:
35
36 333 Shorte, S. L., Frischknecht, F. (Eds.), *Imaging Cellular and Molecular Biological*
37
38 334 *Functions*, Springer, Heidelberg 2007, pp. 289- 312.
39
40
41 335 [15] Patterson, G. H., Piston, D. W., Photobleaching in Two-Photon Excitation
42
43 336 Microscopy. *Biophys J* 2000, 78, 2159-2162.
44
45
46 337 [16] Diaspro, A., Chirico, G., Collini, M., Two-Photon Fluorescence Excitation and
47
48 338 Related Techniques in Biological Microscopy. *Q Rev Biophys* 2005, 38, 97-166.
49
50
51 339 [17] Tauer, U., Advantages and Risks of Multiphoton Microscopy in Physiology. *Exp*
52
53 340 *Physiol* 2002, 87, 709-714.
54
55
56
57
58
59
60

- 1
2
3 341 [18] Bewersdorf, J., Pick, R., Hell, S. W., Multifocal Multiphoton Microscopy. *Opt Lett*
4
5 342 1998, 23, 655-657.
6
7
8 343 [19] Nielsen, T., Fricke, M., Hellweg, D., Andresen, P., High Efficiency Beam Splitter
9
10 344 for Multifocal Multiphoton Microscopy. *J Microsc* 2001, 201, 368-376.
11
12 345 [20] Dunn, K. W., Sandoval, R. M., Kelly, K. J., Dagher, P. C., *et al.*, Functional Studies
13
14 346 of the Kidney of Living Animals Using Multicolor Two-Photon Microscopy. *Am J*
15
16 347 *Physiol Cell Physiol* 2002, 283, C905-916.
17
18 348 [21] Germain, R. N., Miller, M. J., Dustin, M. L., Nussenzweig, M. C., Dynamic Imaging
19
20 349 of the Immune System: Progress, Pitfalls and Promise. *Nat Rev Immunol* 2006, 6, 497-
21
22 350 507.
23
24 351 [22] Resau, J. H., Sakamoto, K., Cottrell, J. R., Hudson, E. A., Meltzer, S. J., Explant
25
26 352 Organ Culture: A Review. *Cytotechnology* 1991, 7, 137-149.
27
28 353 [23] Denk, W., Delaney, K. R., Gelperin, A., Kleinfeld, D., *et al.*, Anatomical and
29
30 354 Functional Imaging of Neurons Using 2-Photon Laser Scanning Microscopy. *J Neurosci*
31
32 355 *Methods* 1994, 54, 151-162.
33
34 356 [24] Helmchen, F., Waters, J., Ca²⁺ Imaging in the Mammalian Brain in Vivo. *Eur J*
35
36 357 *Pharmacol* 2002, 447, 119-129.
37
38 358 [25] Kleinfeld, D., Mitra, P. P., Helmchen, F., Denk, W., Fluctuations and Stimulus-
39
40 359 Induced Changes in Blood Flow Observed in Individual Capillaries in Layers 2 through 4
41
42 360 of Rat Neocortex. *Proc Natl Acad Sci U S A* 1998, 95, 15741-15746.
43
44 361 [26] Bajenoff, M., Germain, R. N., Seeing Is Believing: A Focus on the Contribution of
45
46 362 Microscopic Imaging to Our Understanding of Immune System Function. *Eur J Immunol*
47
48 363 2007, 37 Suppl 1, S18-33.
49
50
51
52
53
54
55
56
57
58
59
60

- 1
2
3 364 [27] Garside, P., Brewer, J. M., Real-Time Imaging of the Cellular Interactions
4
5 365 Underlying Tolerance, Priming, and Responses to Infection. *Immunol Rev* 2008, 221,
6
7 366 130-146.
8
9
10 367 [28] Mempel, T. R., Scimone, M. L., Mora, J. R., von Andrian, U. H., In Vivo Imaging of
11
12 368 Leukocyte Trafficking in Blood Vessels and Tissues. *Curr Opin Immunol* 2004, 16, 406-
13
14 369 417.
15
16
17 370 [29] Coudrier, E., Amblard, F., Zimmer, C., Roux, P., *et al.*, Myosin Ii and the Gal-
18
19 371 Galnac Lectin Play a Crucial Role in Tissue Invasion by *Entamoeba Histolytica*. *Cell*
20
21 372 *Microbiol* 2005, 7, 19-27.
22
23
24 373 [30] Hickman, H. D., Bennink, J. R., Yewdell, J. W., Caught in the Act: Intravital
25
26 374 Multiphoton Microscopy of Host-Pathogen Interactions. *Cell Host Microbe* 2009, 5, 13-
27
28 375 21.
29
30
31 376 [31] Konjufca, V., Miller, M. J., "Two-Photon Microscopy of Host-Pathogen
32
33 377 Interactions: Acquiring a Dynamic Picture of Infection in Vivo". *Cell Microbiol* 2009.
34
35
36 378 [32] Melican, K., Richter-Dahlfors, A., Real-Time Live Imaging to Study Bacterial
37
38 379 Infections in Vivo. *Curr Opin Microbiol* 2009, 12, 31-36.
39
40
41 380 [33] El-Achkar, T. M., Huang, X., Plotkin, Z., Sandoval, R. M., *et al.*, Sepsis Induces
42
43 381 Changes in the Expression and Distribution of Toll-Like Receptor 4 in the Rat Kidney.
44
45 382 *Am J Physiol Renal Physiol* 2006, 290, F1034-1043.
46
47
48 383 [34] Gupta, A., Rhodes, G. J., Berg, D. T., Gerlitz, B., *et al.*, Activated Protein C
49
50 384 Ameliorates Lps-Induced Acute Kidney Injury and Downregulates Renal Inos and
51
52 385 Angiotensin 2. *Am J Physiol Renal Physiol* 2007, 293, F245-254.
53
54
55
56
57
58
59
60

- 1
2
3 386 [35] Mansson, L. E., Melican, K., Boekel, J., Sandoval, R. M., *et al.*, Real-Time Studies
4
5 387 of the Progression of Bacterial Infections and Immediate Tissue Responses in Live
6
7 388 Animals. *Cell Microbiol* 2007, 9, 413-424.
8
9
10 389 [36] Hautefort, I., Proenca, M. J., Hinton, J. C., Single-Copy Green Fluorescent Protein
11
12 390 Gene Fusions Allow Accurate Measurement of Salmonella Gene Expression in Vitro and
13
14 391 During Infection of Mammalian Cells. *Appl Environ Microbiol* 2003, 69, 7480-7491.
15
16
17 392 [37] Melican, K., Boekel, J., Mansson, L. E., Sandoval, R. M., *et al.*, Bacterial Infection-
18
19 393 Mediated Mucosal Signalling Induces Local Renal Ischaemia as a Defence against
20
21 394 Sepsis. *Cell Microbiol* 2008, 10, 1987-1998.
22
23
24 395 [38] Chieppa, M., Rescigno, M., Huang, A. Y., Germain, R. N., Dynamic Imaging of
25
26 396 Dendritic Cell Extension into the Small Bowel Lumen in Response to Epithelial Cell Tlr
27
28 397 Engagement. *J Exp Med* 2006, 203, 2841-2852.
29
30
31 398 [39] Egen, J. G., Rothfuchs, A. G., Feng, C. G., Winter, N., *et al.*, Macrophage and T Cell
32
33 399 Dynamics During the Development and Disintegration of Mycobacterial Granulomas.
34
35 400 *Immunity* 2008, 28, 271-284.
36
37
38 401 [40] Zinselmeyer, B. H., Lynch, J. N., Zhang, X., Aoshi, T., Miller, M. J., Video-Rate
39
40 402 Two-Photon Imaging of Mouse Footpad - a Promising Model for Studying Leukocyte
41
42 403 Recruitment Dynamics During Inflammation. *Inflamm Res* 2008, 57, 93-96.
43
44
45 404 [41] Aoshi, T., Zinselmeyer, B. H., Konjufca, V., Lynch, J. N., *et al.*, Bacterial Entry to
46
47 405 the Splenic White Pulp Initiates Antigen Presentation to Cd8+ T Cells. *Immunity* 2008,
48
49 406 29, 476-486.
50
51
52 407 [42] Amino, R., Menard, R., Frischknecht, F., In Vivo Imaging of Malaria Parasites--
53
54 408 Recent Advances and Future Directions. *Curr Opin Microbiol* 2005, 8, 407-414.
55
56
57
58
59
60

- 1
2
3 409 [43] Frischknecht, F., Baldacci, P., Martin, B., Zimmer, C., *et al.*, Imaging Movement of
4
5
6 410 Malaria Parasites During Transmission by Anopheles Mosquitoes. *Cell Microbiol* 2004,
7
8 411 6, 687-694.
9
10 412 [44] Vlachou, D., Zimmermann, T., Cantera, R., Janse, C. J., *et al.*, Real-Time, in Vivo
11
12 413 Analysis of Malaria Ookinete Locomotion and Mosquito Midgut Invasion. *Cell*
14
15 414 *Microbiol* 2004, 6, 671-685.
16
17 415 [45] Frevert, U., Engelmann, S., Zougbede, S., Stange, J., *et al.*, Intravital Observation of
18
19 416 Plasmodium Berghei Sporozoite Infection of the Liver. *PLoS Biol* 2005, 3, e192.
20
21 417 [46] Tarun, A. S., Baer, K., Dumpit, R. F., Gray, S., *et al.*, Quantitative Isolation and in
22
23 418 Vivo Imaging of Malaria Parasite Liver Stages. *Int J Parasitol* 2006, 36, 1283-1293.
24
25 419 [47] Thiberge, S., Blazquez, S., Baldacci, P., Renaud, O., *et al.*, In Vivo Imaging of
26
27 420 Malaria Parasites in the Murine Liver. *Nat Protoc* 2007, 2, 1811-1818.
28
29 421 [48] Millington, O. R., Gibson, V. B., Rush, C. M., Zinselmeyer, B. H., *et al.*, Malaria
30
31 422 Impairs T Cell Clustering and Immune Priming Despite Normal Signal 1 from Dendritic
32
33 423 Cells. *PLoS Pathog* 2007, 3, 1380-1387.
34
35 424 [49] Bajenoff, M., Breart, B., Huang, A. Y., Qi, H., *et al.*, Natural Killer Cell Behavior in
36
37 425 Lymph Nodes Revealed by Static and Real-Time Imaging. *J Exp Med* 2006, 203, 619-
38
39 426 631.
40
41 427 [50] Peters, N. C., Egen, J. G., Secundino, N., Debrabant, A., *et al.*, In Vivo Imaging
42
43 428 Reveals an Essential Role for Neutrophils in Leishmaniasis Transmitted by Sand Flies.
44
45 429 *Science* 2008, 321, 970-974.
46
47 430 [51] Chtanova, T., Schaeffer, M., Han, S. J., van Dooren, G. G., *et al.*, Dynamics of
48
49 431 Neutrophil Migration in Lymph Nodes During Infection. *Immunity* 2008, 29, 487-496.
50
51
52
53
54
55
56
57
58
59
60

- 1
2
3 432 [52] Junt, T., Moseman, E. A., Iannaccone, M., Massberg, S., *et al.*, Subcapsular Sinus
4
5
6 433 Macrophages in Lymph Nodes Clear Lymph-Borne Viruses and Present Them to
7
8 434 Antiviral B Cells. *Nature* 2007, *450*, 110-114.
9
10 435 [53] Hickman, H. D., Takeda, K., Skon, C. N., Murray, F. R., *et al.*, Direct Priming of
11
12 436 Antiviral Cd8+ T Cells in the Peripheral Interfollicular Region of Lymph Nodes. *Nat*
13
14 437 *Immunol* 2008, *9*, 155-165.
15
16 438 [54] Kim, J. V., Kang, S. S., Dustin, M. L., McGavern, D. B., Myelomonocytic Cell
17
18 439 Recruitment Causes Fatal Cns Vascular Injury During Acute Viral Meningitis. *Nature*
19
20 440 2009, *457*, 191-195.
21
22 441 [55] Tanner, G. A., Sandoval, R. M., Molitoris, B. A., Bamburg, J. R., Ashworth, S. L.,
23
24 442 Micropuncture Gene Delivery and Intravital Two-Photon Visualization of Protein
25
26 443 Expression in Rat Kidney. *Am J Physiol Renal Physiol* 2005, *289*, F638-643.
27
28 444 [56] Bao, H., Allen, J., Pattie, R., Vance, R., Gu, M., Fast Handheld Two-Photon
29
30 445 Fluorescence Microendoscope with a 475 Microm X 475 Microm Field of View for in
31
32 446 Vivo Imaging. *Opt Lett* 2008, *33*, 1333-1335.
33
34 447 [57] Kim, P., Puoris'haag, M., Cote, D., Lin, C. P., Yun, S. H., In Vivo Confocal and
35
36 448 Multiphoton Microendoscopy. *J Biomed Opt* 2008, *13*, 010501.
37
38 449 [58] Ashworth, S. L., Sandoval, R. M., Tanner, G. A., Molitoris, B. A., Two-Photon
39
40 450 Microscopy: Visualization of Kidney Dynamics. *Kidney Int* 2007, *72*, 416-421.
41
42 451 [59] Ando, R., Hama, H., Yamamoto-Hino, M., Mizuno, H., Miyawaki, A., An Optical
43
44 452 Marker Based on the Uv-Induced Green-to-Red Photoconversion of a Fluorescent
45
46 453 Protein. *Proc Natl Acad Sci U S A* 2002, *99*, 12651-12656.
47
48
49
50
51
52
53
54
55
56
57
58
59
60

- 1
2
3 454 [60] Gurskaya, N. G., Verkhusha, V. V., Shcheglov, A. S., Staroverov, D. B., *et al.*,
4
5 455 Engineering of a Monomeric Green-to-Red Photoactivatable Fluorescent Protein Induced
6
7 456 by Blue Light. *Nat Biotechnol* 2006, 24, 461-465.
8
9
10 457 [61] Kedrin, D., Gligorijevic, B., Wyckoff, J., Verkhusha, V. V., *et al.*, Intravital Imaging
11
12 458 of Metastatic Behavior through a Mammary Imaging Window. *Nat Methods* 2008, 5,
13
14 459 1019-1021.
15
16 460 [62] Liu, W., Howarth, M., Greytak, A. B., Zheng, Y., *et al.*, Compact Biocompatible
17
18 461 Quantum Dots Functionalized for Cellular Imaging. *J Am Chem Soc* 2008, 130, 1274-
19
20 462 1284.
21
22 463 [63] Zhou, M., Ghosh, I., Quantum Dots and Peptides: A Bright Future Together.
23
24 464 *Biopolymers* 2007, 88, 325-339.
25
26
27 465
28
29 466
30
31
32
33
34
35
36
37
38
39
40
41
42
43
44
45
46
47
48
49
50
51
52
53
54
55
56
57
58
59
60

1
2
3 467 **Figure Legends**

4 468

5
6 469 **Figure 1**

7
8 470 Jablonski diagram showing the energetic states of a fluorophore. Fluorescence is emitted
9
10 471 when a fluorophore absorbs light at a particular wavelength, gets moved to its excitation
11
12 472 state and after a brief interval, termed the fluorescence lifetime, returns to its ground
13
14
15 473 state, emitting light. A 400nm single photon excitation (left) will excite a fluorophore
16
17 474 such as FITC. In two-photon excitation, two lower-energy photons of a wavelength of
18
19
20 475 around 800 nm combine to excite FITC (right).

21
22 476

23 477

24
25 478 **Figure 2**

26 479

27 480 MPM of bacteria-host interaction. UPEC infection in the kidney. Example images show
28
29 481 the spatial resolution possible when using MPM. Infection site shown 1.5 h post bacterial
30
31
32 482 infusion into the kidney (left). Injected proximal tubules (Pt) are outlined with a co-
33
34 483 injected 10 kDa dextran conjugated to cascade blue, which is endocytosed by the
35
36 484 proximal tubule cells (blue). Cellular nuclei are labeled with Hoechst 33342 (cyan) and
37
38 485 blood plasma with a 500 kDa dextran conjugated to tetramethylrhodamine (red). Red
39
40 486 blood cells can be seen as black silhouettes in the red stained plasma within the vessels.
41
42
43
44 487 No bacteria are visible at this early time point. The endogenous autofluorescence of
45
46 488 proximal tubules cells is seen as a dull green in non-injected tubules. 5 h post infection
47
48 489 (center) a few bacteria can be seen adhering to the epithelial lining of proximal tubule
49
50 490 (arrow, bright green). Despite the low numbers of bacteria seen in this particular image
51
52
53 491 vascular shutdown can be noted by the loss of red dextran. Different view of same
54
55 492 infected nephron showing heavy bacterial colonization (bright green) of proximal tubules
56
57
58
59
60

1
2
3 493 at 8.5 h (right). Blood flow in the area is greatly compromised as noted by the lack of red
4
5 494 dextran, and RBC flow. Epithelial breakdown is noted by the sloughing of blue dextran
6
7
8 495 labeled epithelial cells into the bacteria filled lumen of the proximal tubule (arrow). A
9
10 496 non-infected proximal tubule can also be seen (*). Scale bar = 30µm.
11
12
13 497

14
15 498 Figure 3. Parasite-host interaction. Neutrophils are rapidly recruited to sites of sand fly
16
17 499 bite. MPM time-lapse images from the ears of LYS-eGFP mice (mice expressing
18
19 500 enhanced green fluorescent protein (eGFP) under the control of the endogenous lysozyme
20
21 501 M promoter) (green) beginning 40 min after exposure to uninfected sand flies (left) or
22
23 502 *Leishmania major* -RFP-infected (red) sand flies (right). Circles represent sites of sand
24
25 503 fly proboscis penetration. Scale bar = 30µm. From [50]. Reprinted with permission from
26
27 504 AAAS.
28
29
30
31

32 505
33
34 506 Figure 4. Viral-host interaction. Capture of lymph-borne vesicular stomatitis virus
35
36 507 (VSV). MPM micrographs of ultraviolet-inactivated VSV (green) in a popliteal lymph
37
38 508 node (LN). Numbers indicate minutes after footpad injection. Tissue structure is shown
39
40 509 by second harmonic generation (blue). Numbers in the left upper corner indicate minutes
41
42 510 and seconds after footpad injection of the virus. Scale bar = 100 µm. Adapted by
43
44 511 permission from Macmillan Publishers Ltd: [Nature] [52] copyright (2007).
45
46
47

48 512
49
50 513
51
52 514
53
54
55 515
56
57
58
59
60

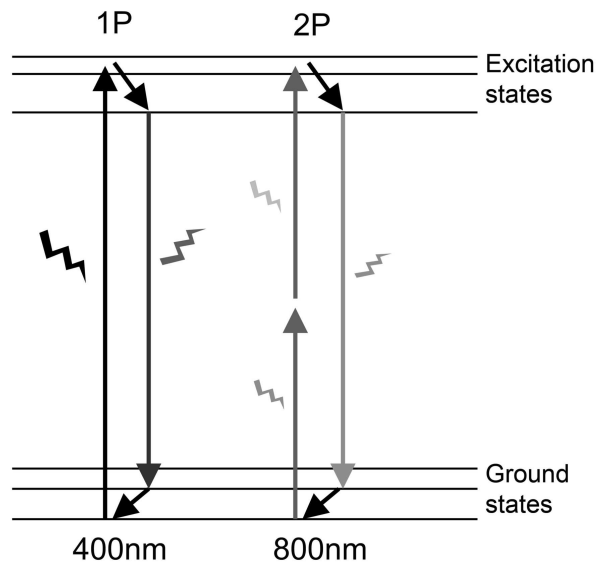
1
2
3 516 [**Agneta Richter-Dahlfors** received her M.Sc. in Molecular Biology 1989 and completed](#)
4
5 517 [her Ph.D. 1994 in Microbiology at Uppsala University, Sweden. She joined](#)
6
7 518 [Biotechnology Laboratories, University of British Columbia, Vancouver, as a post-](#)
8
9 519 [doctoral fellow 1995–1997, developing technologies to visualize bacteria-induced tissue](#)
10
11 520 [rearrangements using rodent infection models. In 1998, she was recruited to Karolinska](#)
12
13 521 [Institutet, Stockholm, where she became Professor in cellular microbiology. She is](#)
14
15 522 [currently pioneering a novel research area, termed “tissue microbiology”, where MPM,](#)
16
17 523 [molecular techniques, and recordings of various physiological functions, are combined to](#)
18
19 524 [visualize in real-time the immediate/early alteration of the tissue homeostasis that](#)
20
21 525 [accompanies bacterial infections. Richter-Dahlfors is engaged in interdisciplinary](#)
22
23 526 [research projects. As co-director of the Strategic Research Centre for Organic](#)
24
25 527 [Bioelectronics \(OBOE\), she is integrating organic electronic technologies in biological](#)
26
27 528 [applications. She was recently appointed director for the Swedish Medical Nanoscience](#)
28
29 529 [Center at Dept of Neuroscience, Karolinska Institutet.](#)

30
31 531 [**Keira Melican** received her B.Sc. from Monash University, Australia in 2004 and](#)
32
33 532 [completed her M.Sc. at Uppsala University, Sweden in 2005. She has been a graduate](#)
34
35 533 [student in the lab of Prof. Agneta Richter-Dahlfors since 2005. Her research interest is](#)
36
37 534 [focused on the analysis of the early tissue responses occurring during the bacterial](#)
38
39 535 [infection process. To achieve this, she has explored the use of MPM-based live imaging](#)
40
41 536 [of the kidney as a means to analyze tissue responses to uropathogenic *Escherichia coli*](#)
42
43 537 [induced infection in the renal cortex.](#)

44
45 538
46
47
48
49
50
51
52
53
54
55
56
57
58
59
60 539

1
2
3
4
5
6
7
8
9
10
11
12
13
14
15
16
17
18
19
20
21
22
23
24
25
26
27
28
29
30
31
32
33
34
35
36
37
38
39
40
41
42
43
44
45
46
47
48
49
50
51
52
53
54
55
56
57
58
59
60

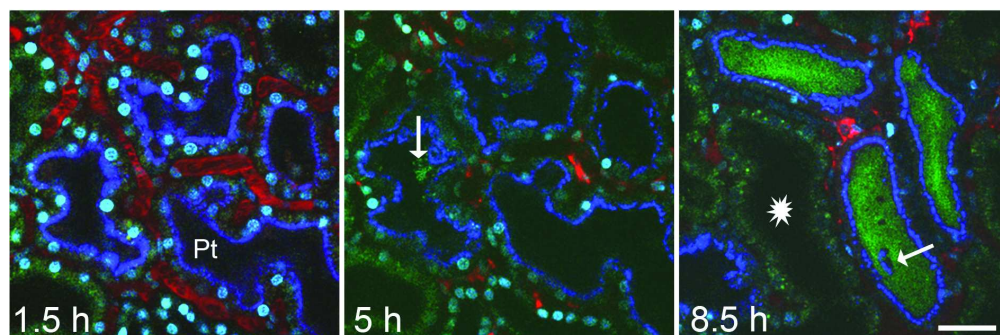
Figure 1



126x127mm (600 x 600 DPI)



Figure 2

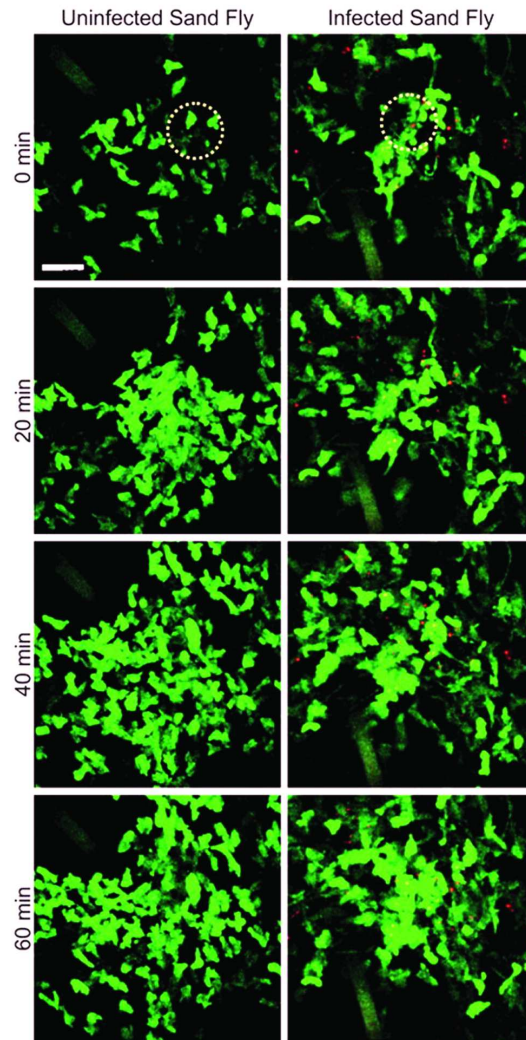


160x73mm (300 x 300 DPI)

Peer Review

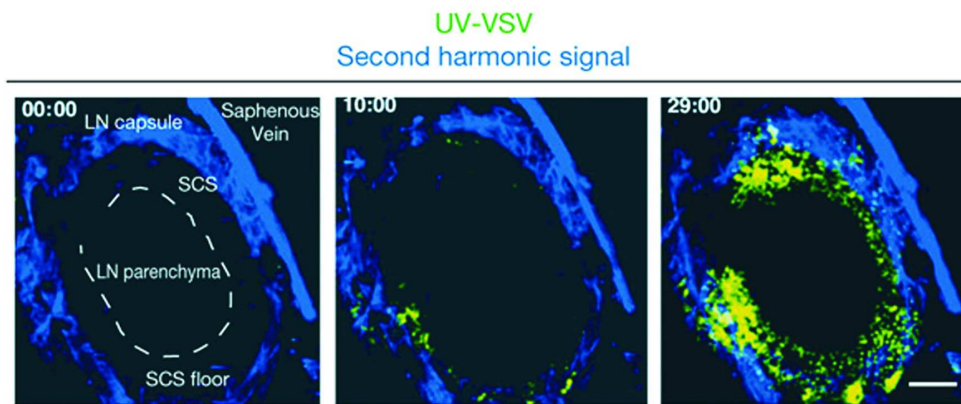
1
2
3
4
5
6
7
8
9
10
11
12
13
14
15
16
17
18
19
20
21
22
23
24
25
26
27
28
29
30
31
32
33
34
35
36
37
38
39
40
41
42
43
44
45
46
47
48
49
50
51
52
53
54
55
56
57
58
59
60

Figure 3



84x187mm (300 x 300 DPI)

Figure 4



152x77mm (300 x 300 DPI)

1
2
3
4
5
6
7
8
9
10
11
12
13
14
15
16
17
18
19
20
21
22
23
24
25
26
27
28
29
30
31
32
33
34
35
36
37
38
39
40
41
42
43
44
45
46
47
48
49
50
51
52
53
54
55
56
57
58
59
60



99x111mm (300 x 300 DPI)

1
2
3
4
5
6
7
8
9
10
11
12
13
14
15
16
17
18
19
20
21
22
23
24
25
26
27
28
29
30
31
32
33
34
35
36
37
38
39
40
41
42
43
44
45
46
47
48
49
50
51
52
53
54
55
56
57
58
59
60



99x118mm (300 x 300 DPI)